Bulletin of the Seismological Society of America, Vol. 105, No. 6, pp. 3156–3166, December 2015, doi: 10.1785/0120150078

Applicability of the Multiple-Event Stacking Technique for Shear-Wave Splitting Analysis

by Fansheng Kong, Stephen S. Gao, and Kelly H. Liu

Abstract For several decades, shear-wave splitting (SWS) parameters (fast polarization orientations and splitting times) have been widely measured to reveal the orientation and strength of mantle anisotropy. One of the most popularly used techniques for obtaining station-averaged SWS parameters is the multiple-event stacking technique (MES). Results from previous studies suggest the splitting times obtained using MES are frequently smaller than those derived from simple averaging of splitting times obtained using the event-specific technique of Silver and Chan (1991). To confirm such apparent discrepancies between the two popularly used methods and to explore the causes, we conduct numerical experiments using both synthetic and observed data. The results show that when the anisotropic structure can be represented by a horizontal single layer of anisotropy with constant or spatially varying splitting times, MES can accurately retrieve the splitting parameters. However, when the fast orientations or both splitting parameters vary azimuthally due to lateral heterogeneities or double-layer anisotropy, the station-averaged fast orientations from MES and Silver and Chan (1991) are mostly comparable, but the splitting times obtained using MES are underestimated. For laterally varying fast orientations in the vicinity of a station, the magnitude of the underestimation is dependent on the arriving azimuth of the events participated in the stacking; for two-layer models of anisotropy, the resulting splitting parameters using MES are biased toward those of the top layer, due to the dominance of events with a back azimuth parallel or orthogonal to the fast orientation of the lower layer.

Introduction

Shear-wave splitting (SWS) analyses have been increasingly used by geoscientists as an important tool in studying seismic anisotropy, which is directly related to the deformation and dynamics of the Earth's interior (Fuchs, 1977; Ando *et al.*, 1983; Silver and Chan, 1991; Silver, 1996; Silver and Holt, 2002; Becker, 2008; Gao and Liu, 2009; Gao *et al.* 2010; Long and Becker, 2010; Yang *et al.*, 2014). The splitting parameters, fast polarization orientation (ϕ), and splitting time (δt) convey information about the direction and strength, respectively, of finite strain. A number of techniques aimed at accurately retrieving the splitting parameters using *P*-to-*S* converted phases at the core–mantle boundary (*XKS*, including *SKS*, *SKKS*, and *PKS*) have been developed to quantify seismic anisotropy beneath the recording stations (Ando *et al.*, 1983; Vinnik *et al.*, 1989; Silver and Chan, 1991; Wolfe and Silver, 1998; Levin *et al.*, 1999; Restivo and Helffrich, 1999; Chevrot, 2000).

Among these techniques, arguably the most popularly used one is the transverse energy minimization method (Silver and Chan, 1991; hereafter referred to as SC). For each event recorded by a station, SC grid searches for the optimal pair of splitting parameters corresponding to the minimum value on the contour map for the energy of the corrected transverse component. In most previous studies, the splitting parameters from individual events are then averaged to obtain a mean pair of splitting parameters for the station. Another widely used approach to obtain station-averaged splitting parameters is the multiple-event stacking technique (MES) proposed by Vinnik *et al.* (1989) and modified by Wolfe and Silver (1998). It was initially designed to obtain splitting parameters using noisy teleseismic data such as those recorded by ocean island stations, at which SC could not lead to reliable measurements due to the high noise level. MES is also effective for situations when the splitting time is significantly smaller than the global average of 1.0 s or when the fast or slow orientation is close to the back azimuth of the event. Restivo and Helffrich (1999) proposed a revised version of the approach of Wolfe and Silver (1998) by introducing two weighting factors to place emphasis on high-quality signals and to partially correct for uneven distributions in the back azimuth of the *XKS* events recorded by the station.

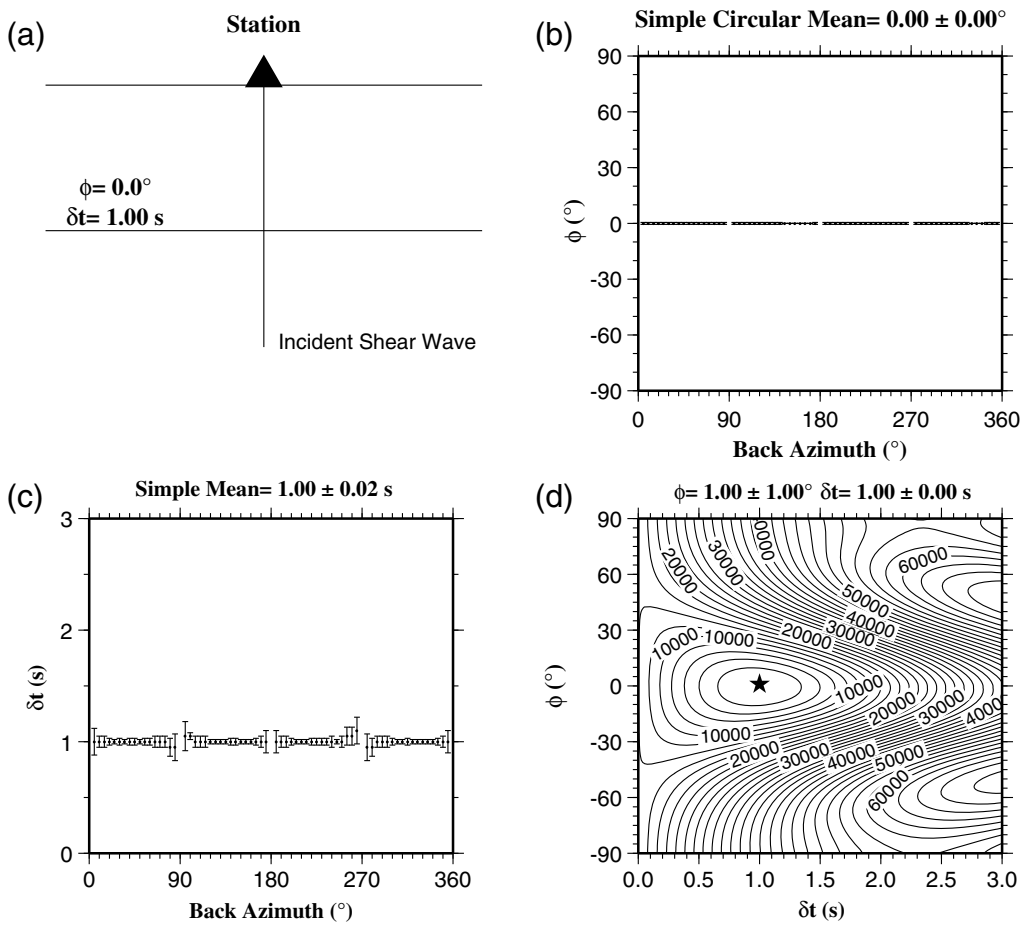

Figure 1. A model of homogeneous simple anisotropy and results of synthetic tests. (a) The model. (b) Fast orientations obtained using Silver and Chan (1991, hereafter referred to as SC). (c) Splitting times using SC. (d) Contour map of the stacked misfit function and resulting splitting parameters calculated by multiple-event stacking technique (MES). The star indicates the optimal pair of splitting parameters corresponding to minimum transverse energy.

Although splitting parameters estimated by MES usually have a smaller 95% confidence interval than those obtained using SC (Wolfe and Silver, 1998; Restivo and Helffrich, 1999), numerous measurements using both techniques at the same stations suggest the splitting times estimated by MES are systematically lower than those from averaging the event-specific measurements using SC. For instance, at station QIZ (Hainan Island, China), Bai *et al.* (2009) reported a station-averaged δt of 0.88 s using MES but 1.28 s using SC. Similarly, the same study revealed a δt of 1.08 s at station SPVO (Vietnam) using MES and 1.66 s using SC. This discrepancy was highlighted in two recent SWS studies using hundreds of broadband seismic stations in the western United States. The study of Liu *et al.* (2014) used SC and reported a mean δt of 1.33 s for the western United States orogenic zone, whereas that of Walpole *et al.* (2014), which used MES and the covariance matrix eigenvalue minimization method of Silver and Chan (1991), reported a value of 1.08 s. Several dramatic examples include USArray Transportable Array (TA) station 433A (Art, Texas) at which Walpole *et al.* (2014) obtained a δt of 0.3 s and Liu *et al.* (2014) reported a value of 1.3 s; at 435B (Jarrell, Texas), the corresponding values are 0.47 and 1.1 s, whereas at ANMO (Albuquerque, New Mexico), the values are 0.72 and 1.6 s. Globally, the Walpole *et al.* (2014) study reported a mean δt of 0.8 s, which is smaller than the global average of 1.0 s obtained by Silver (1996) and the 1.1 s from a global compilation of SWS measurements by Becker *et al.* (2012). Such differences may lead to conflicting implications of mantle deformation and dynamics, especially when the splitting parameters are used in geodynamic modeling (e.g., Becker, 2008) and as constraints for seismic tomography (Yuan and Romanowicz, 2010).

In this study, we use both synthetic and observed seismograms to test if the discrepancies were the results of normal fluctuations among different studies or were caused by a systematic underestimation of δt by MES (or, alternatively, a systematic overestimation by SC). We use several anisotropy models, including a single homogeneous anisotropy layer, spatially varying single-layer anisotropy in the vicinity of a station, and a model with two anisotropic layers for the

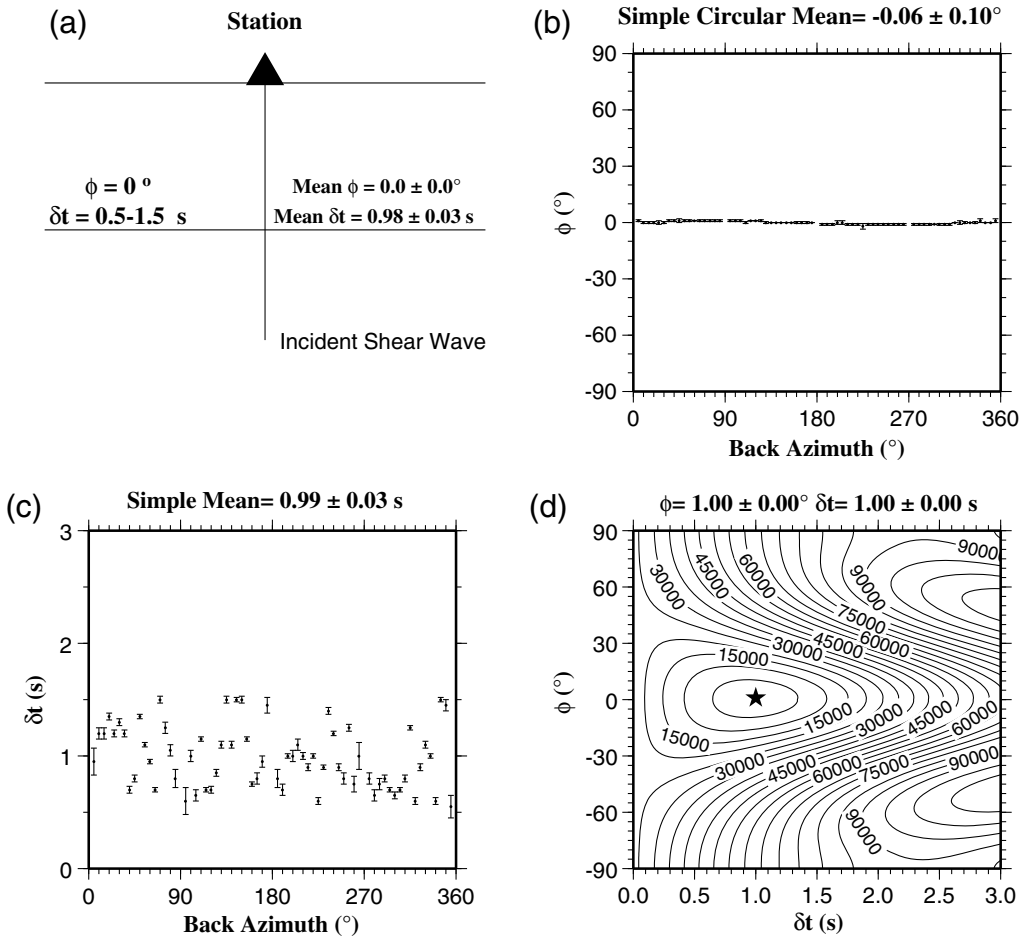

Figure 2. Same as Figure 1 but for a model of anisotropy with δt values randomly distributed in the 0.5–1.5 s range.

synthetic tests. We also measured splitting parameters using both techniques for two broadband stations, one with spatially varying ϕ values in the vicinity of the station and the other being characterized by systematic azimuthal variations of individual splitting parameters.

Measuring Technique

For each of the events recorded by a station, MES first computes the *XKS* energy on the corrected transverse component as a function of the candidate ϕ and δt, using SC. Following Restivo and Helffrich (1999), in this study we refer to the resulting function as a misfit function. Each misfit function is then normalized by its minimum value, and a stacked misfit function for the station is obtained using

$$S(\phi_i, \delta t_j) = \sum_{m=1}^{N} F_m(\phi_i, \delta t_j) / \min(F_m) \qquad (1)$$

(Wolfe and Silver, 1998), in which $S(\phi_i, \delta t_j)$ is the stacked misfit function at the candidate pair of splitting parameters $(\phi_i, \delta t_j)$, N is the number of events recorded by the station, and $F_m(\phi_i, \delta t_j)/\min(F_m)$ is the normalized misfit function of the mth event at the candidate pair of splitting parameters.

To give higher-quality events a higher weighting factor in the stacking, Restivo and Helffrich (1999) modified this technique to multiply the individual misfit functions by the signal-to-noise ratio (SNR) on the radial component before stacking. In addition, to avoid dominance of too many events from narrow back-azimuth ranges, the misfit function is also divided by the number of events in the back-azimuth range to which the event belongs, before being used for stacking. In the following, we apply the modified version of MES proposed by Restivo and Helffrich (1999). We define the SNR as $\max|A_{(a,f)}|/\max|A_{(a-10,a)}|$, in which $\max|A_{(a,f)}|$ is the maximum absolute value between a and f (the beginning and end of the *XKS* window in seconds) on the radial component and $\max|A_{(a-10,a)}|$ is that between $a-10$ and a seconds. Because the back azimuths of the hypothetical events used for the synthetic tests are evenly distributed and the SNR on the radial component is the same for all the events, the two weighting factors have no effects on the synthetic tests in the study. They are applied in the tests using observed data. Also, to obtain reliable event-specific splitting measurements,

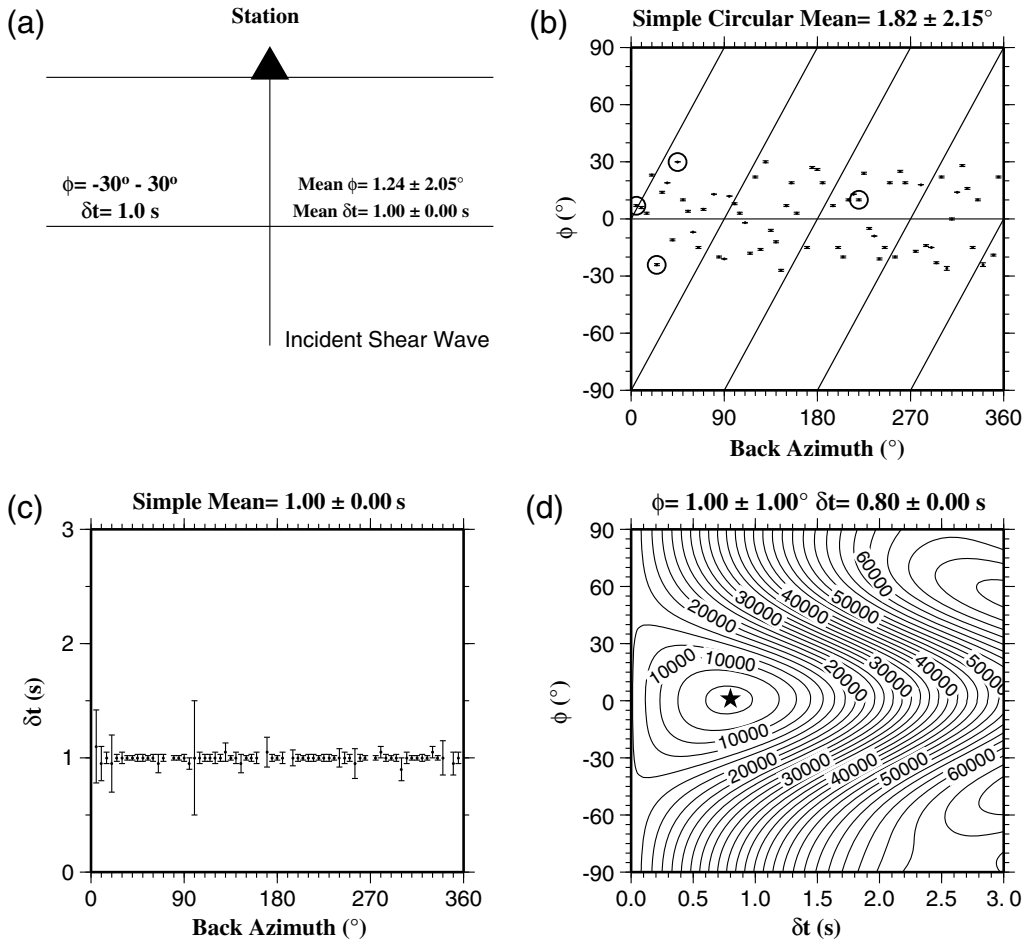

Figure 3. Same as Figure 1 but for a model of anisotropy with ϕ values randomly distributed in the −30° to 30° range. (b) The tilted lines indicate the situation of ϕ = back azimuth $\pm\, n \times 90°$ (or $\beta = 0°$), in which n is an integer. The misfit functions of the four events highlighted by black circles are shown in Figure 5.

manual checking and necessary adjustments of the measuring parameters (such as the a and f values and results of autoranking) are required. Details of the procedure for measuring event-specific splitting parameters using SC can be found in Liu and Gao (2013).

Synthetic Tests

Synthetic Data Generation

To construct a simple anisotropy model composed of a single layer of anisotropy with a horizontal axis of symmetry, we first define a presplitting radial component as

$$R(t) = A_0 \sin(2\pi f t) e^{-\alpha t}, \tag{2}$$

in which $A_0 = 1.0$ is the amplitude, $f = 0.15$ Hz is the frequency, and $\alpha = 0.2$ is the decaying factor. The fast (S_f) and slow (S_s) components with an incidence angle of 0° traveling through an anisotropic layer with splitting parameters of ϕ and δt can be expressed as

$$S_f(t) = R(t)\cos(\theta) \tag{3}$$

and

$$S_s(t) = -R(t - \delta t)\sin(\theta), \tag{4}$$

in which θ is the angular difference between the radial and the fast orientations. Synthetic seismograms are then produced by rotating $S_f(t)$ and $S_s(t)$ to the north–south and east–west directions, based on the back azimuth of the event. For a two-layer anisotropy model, the fast and slow shear waves after passing the lower layer act as independent incident shear waves and travel through the upper layer. The fast and slow waves after traveling through both layers are summed in the time domain and then rotated to create the north–south and east–west components.

Simple Homogeneous Anisotropy

We first consider a model with a single homogeneous layer of anisotropy with a horizontal axis of symmetry (Fig. 1a). A total of 71 synthetic records with an SNR of 100 were gen-

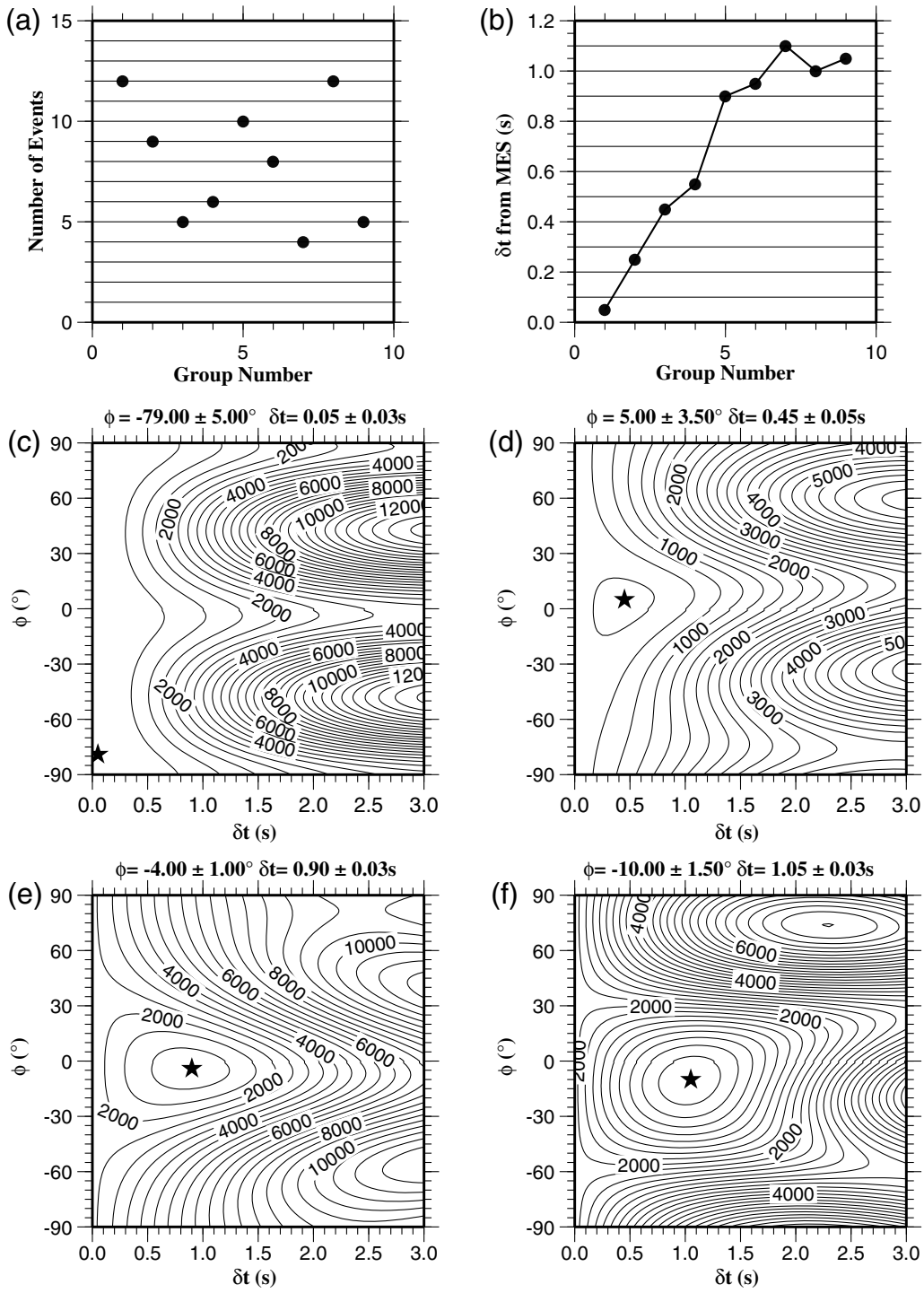

Figure 4. MES measurements using events with different β values. (a) Number of events in each group for groups 1–9. (b) Observed δt of each group obtained by applying MES. (c) Contour map of stacked misfit function and resulting splitting parameters from MES using events in group 1. (d) Same as (c) but for group 3. (e) Same as (c) but for group 5. (f) Same as (c) but for group 9.

erated using the same ϕ of 0° and δt of 1.0 s. The back azimuths of the events range from 5° to 355°, with an interval of 5°. Uncorrelated noise with a prefiltering maximum amplitude of 10% of the incident wave amplitude was created by a random number generator (Press *et al.*, 1992) and was added to the north–south and east–west components after being low-pass filtered (0.3 Hz), and the individual splitting measurements and corresponding misfit functions were obtained by following the SC-based procedure of Liu and Gao (2013).

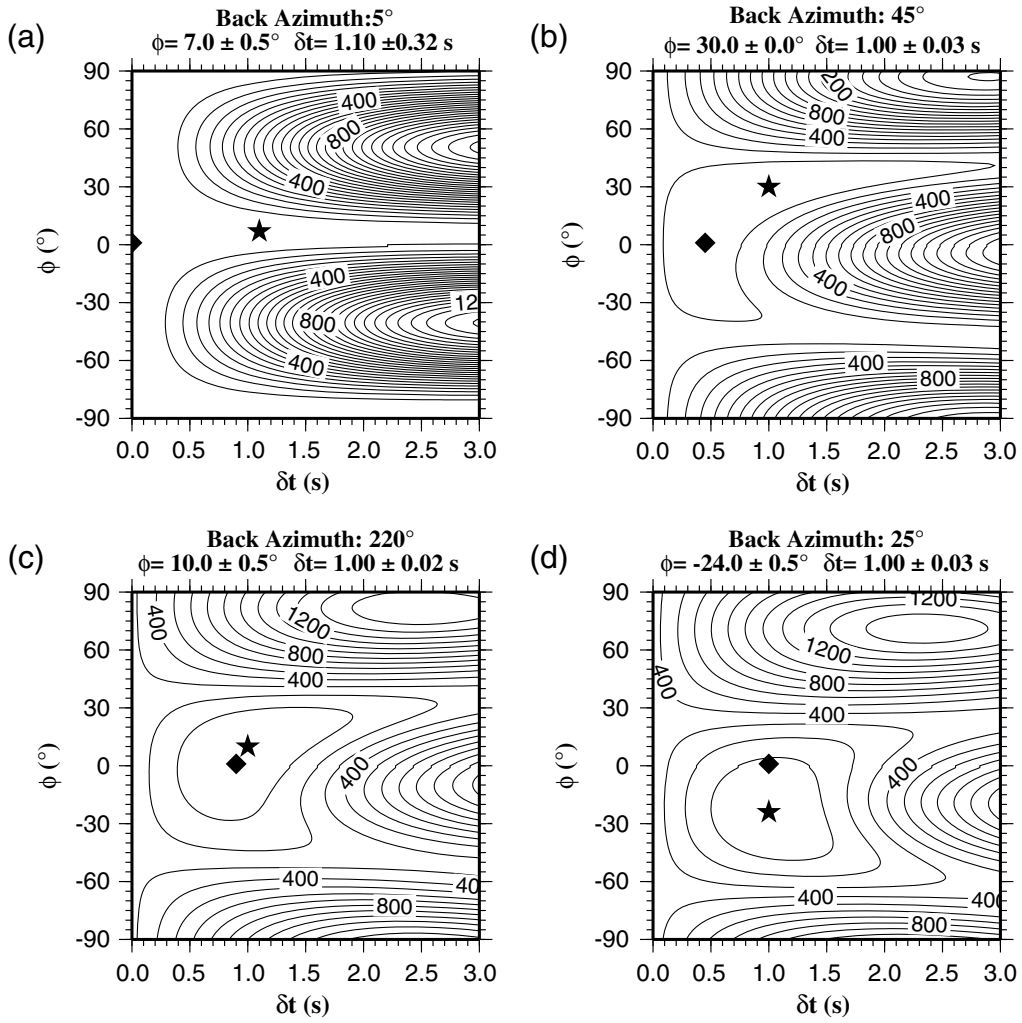

Figure 5. Example misfit functions for the four highlighted events in Figure 3b. The star indicates optimal splitting parameters for each of the events, and the diamond represents the point of minimum transverse energy when $\phi = 1°$, which is the global ϕ from MES. The back azimuth of the event and resulting event-specific parameters are shown at the top of each plot.

The resulting station averages obtained using SC for both ϕ and δt (Fig. 1b,c) are identical to the splitting parameters used for generating the synthetic seismograms. Similarly, when MES is used, the optimal pair of splitting parameters corresponding to the minimum value on the stacked misfit function (Fig. 1d) is also consistent with the true parameters. The high accuracy of the results from MES is easily understandable, because all the individual misfit functions have the same minimum point (0°, 1.0 s). The above tests suggest that both SC and MES can accurately retrieve the splitting parameters when homogeneous simple anisotropy is present.

Laterally Varying Anisotropy

The *XKS* ray paths arriving at a station sample an approximately cone-shaped volume centered at the station. The diameter of the cone increases with depth and can reach a few hundred kilometers in the upper mantle, depending on the angle of incidence as well as the frequency (which determines the size of the Fresnel zone) (Alsina and Snieder, 1995). In such a large area, significant heterogeneities in the orientation and strength of seismic anisotropy are likely to exist. The heterogeneities can lead to inconsistent splitting parameters obtained from different events recorded by the same station, even when the anisotropy can locally be represented by a single layer with a horizontal axis of symmetry (e.g., station ENH in Hubei, China, described in Liu and Gao, 2013). In such a situation, the splitting parameters are dependent on the location of the ray-piercing points and the back azimuth.

The model shown in Figure 2a has a uniform ϕ of 0° but randomly distributed δt in the 0.5–1.5 s range, with a simple mean of 0.98 ± 0.03 s. The application of the SC-based procedure of Liu and Gao (2013) resulted in an average ϕ of −0.06 ± 0.1° and δt of 0.99 ± 0.03 s (Fig. 2b,c), both of

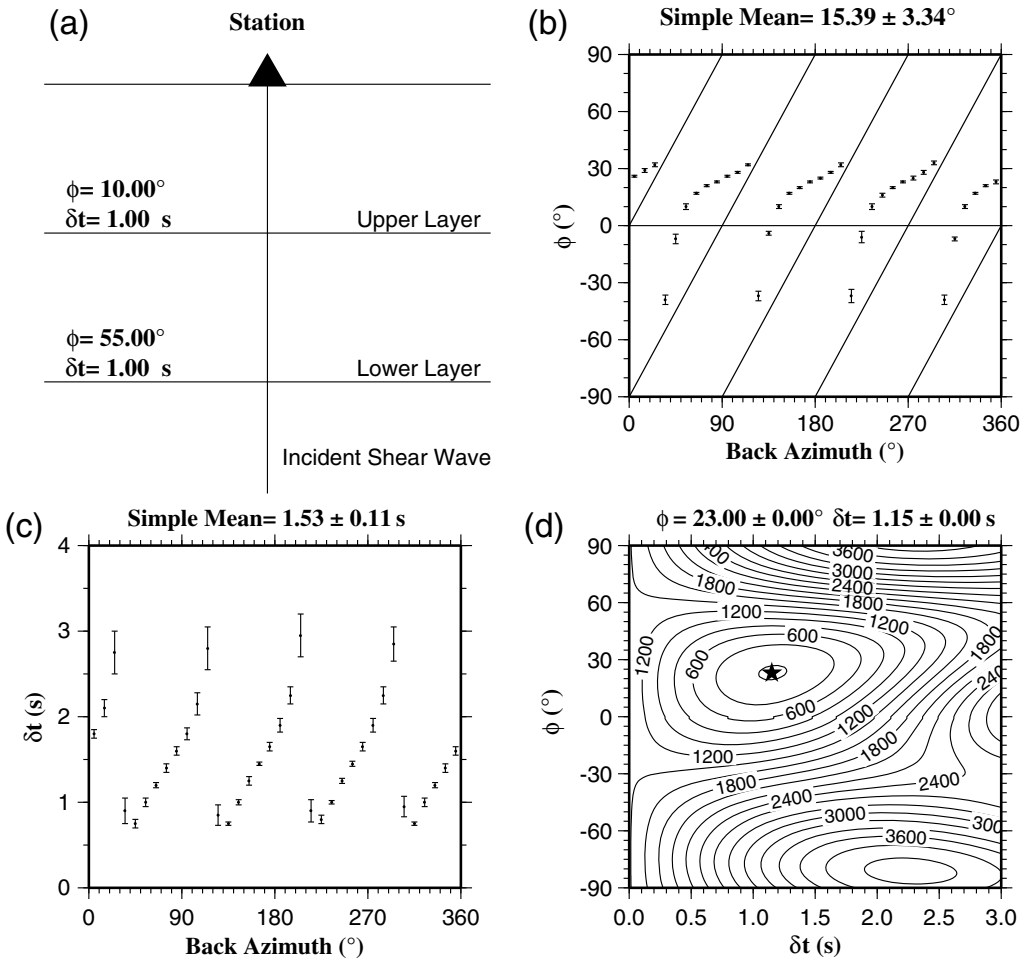

Figure 6. Same as Figure 3 but for a two-layer anisotropy model shown in (a).

which are consistent with the parameters used to generate the synthetic seismograms. Similarly, the resulting optimal ϕ and δt from MES are $1.0 \pm 0.0°$ and 1.0 ± 0.0 s (Fig. 2d), which are also consistent with the expected values. Therefore, both SC and MES can lead to accurate results for the situation of constant ϕ and spatially varying δt.

We next explore the performance of MES for a model with a constant δt of 1.0 s but randomly distributed ϕ in the $-30°$ to $30°$ range (Fig. 3a). The mean of the individual ϕ values used to generate the synthetic seismograms is $1.24° \pm 2.05°$. The SC approach resulted in a station average of $1.82° \pm 2.15°$ for ϕ and 1.0 ± 0.00 for δt (Fig. 3b,c), both of which are consistent with the splitting parameters used to generate the seismograms. Note that 5 of the 71 events produced null results because the fast orientation is nearly parallel or orthogonal to the back azimuth. The resulting ϕ from MES is $1.00° \pm 0.00°$, which is also close to the expected value. However, the resulting δt is 0.80 ± 0.00 s (Fig. 3d), in spite of the fact that the model has a uniform δt of 1.0 s for all the events.

This discrepancy seems counterintuitive and consequently needs additional exploration. To facilitate this task, we first define β, which is the modulo-90° absolute angular difference between the fast orientation and the back azimuth of an event. When β is greater than 45°, it is taken as $90° - \beta$, so that β is limited to the 0°–45° range. For instance, for the first event shown in Figure 3b, $\beta = 2°$ because the event has a back azimuth of 5° and a local ϕ of 7°; for the fifth event, $\beta = 41°$ because the back azimuth is 25° and $\phi = -24°$. Note that $\beta = 0°$ for events along the tilted lines in Figure 3b.

To identify possible relationships between the global δt (i.e., the δt from MES) and the β values of the participating events, we divide the 71 events into nine groups based on the β values. The β value for events in the ith group ranges from $5 \times (i - 1)$ to $5 \times i°$. The number of events for each of the groups is shown in Figure 4a. We then perform MES separately using events from each of the groups. The resulting global δt values increase significantly with increasing β, from as small as 0.05 s for group 1, to 1.0–1.1 s for groups 7–9 (Fig. 4b). Misfit functions for four of the groups are shown in Figure 4c–f.

Such a strong dependence of the global δt on β can be explained using the example misfit functions shown in Figure 5. Although the resulting δt for the individual events (i.e., local δt) is 1.0 s (which was used to generate the synthetics), the δt associated with the minimum energy when $\phi = 1°$

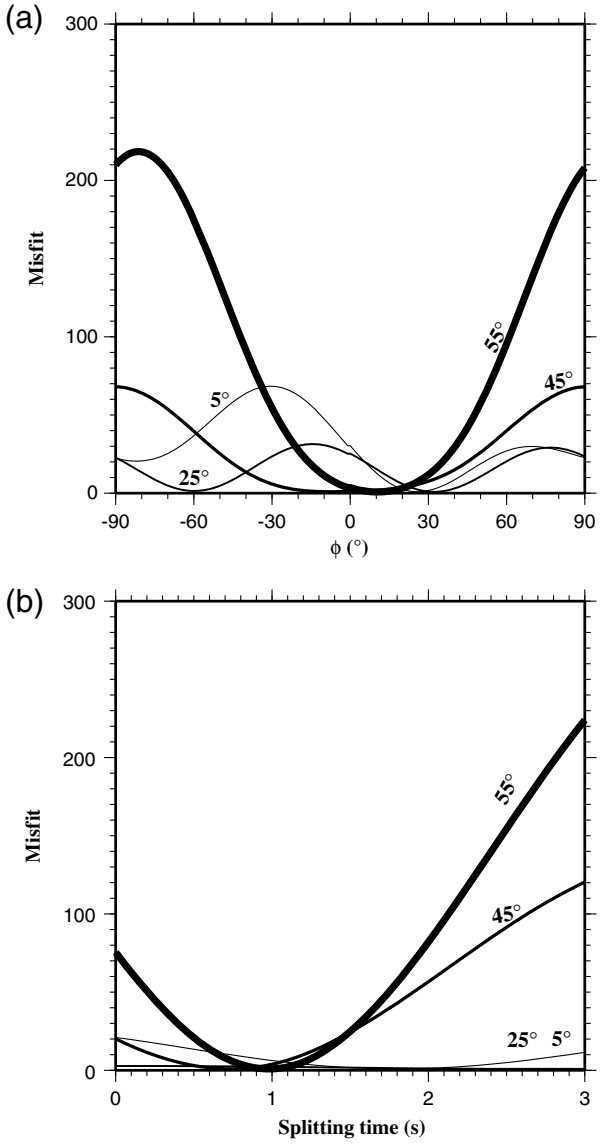

Figure 7. (a) Cross-section plots of example individual misfit functions under the two-layer model shown in Figure 6 along the ϕ axis. (b) Cross-section plots along the δt axis. For both (a) and (b), the cross sections traverse the point with the minimum value in the individual misfit function. Labels near the curves indicate the back azimuth of the *XKS* event. The thickest curves are for the events with a back azimuth parallel to the fast orientation of the lower layer. Note that in the lower plot, the misfits for some of the events are relatively too small to be visually observed.

(which is the global ϕ from MES) is mostly smaller than the local δt. Thus, when the individual misfit functions are stacked, the point with the minimum energy shifts toward a δt value that is smaller than the local δt. The magnitude of the shift increases with decreasing β (Fig. 5).

We also performed similar tests using a model in which both ϕ and δt vary with the back azimuth, and significant underestimation of δt was also observed. The main conclusion from these tests is that when the fast orientations in the vicinity of a station vary spatially, the resulting δt from MES could be significantly underestimated, and the magnitude of the underestimation is dependent on the β values of the events included in the stacking.

Two Anisotropic Layers

The most commonly discussed complex anisotropy model in previous studies consists of two layers of simple anisotropy with nonparallel and nonorthogonal fast orientations. For a two-layer model, the apparent splitting parameters obtained using SC under the assumption of simple anisotropy vary systematically with the back azimuth with a 90° periodicity (Silver and Savage, 1994). As discussed in Liu and Gao (2013) using synthetic data, under such a model, the *XKS* energy on the transverse component cannot be completely removed using SC, except for the special cases when the back azimuth is parallel or orthogonal to the fast orientation of the lower layer. This is because the *XKS* phase from an event with such a back azimuth does not split when traveling through the lower layer; that is, it only splits once instead of twice. Such anisotropy cannot be satisfactorily represented by station-averaged splitting parameters. Unfortunately, due to reasons such as limited back-azimuth coverage and the associated incapability to recognize the existence of complex anisotropy, many previous studies reported station averages (obtained by MES or SC) for areas with complex anisotropy. In the following, we discuss the consequences of such a practice using a two-layer model with $\phi_1 = 55°$, $\delta t_1 = 1.0$ s for the lower layer and $\phi_2 = 10°$, $\delta t_2 = 1.0$ s for the upper layer (Fig. 6a).

As expected, the application of the SC-based procedure of Liu and Gao (2013) resulted in a set of apparent splitting parameters that vary periodically with the back azimuth (Fig. 6b,c). The optimal splitting parameters from MES (Fig. 6d), 23° and 1.15 s, are apparently well defined and, interestingly, are similar to the splitting parameters of the upper layer (10° and 1.0 s). We conducted similar tests using different combinations of the splitting parameters for the two layers, and the resulting optimal splitting parameters using MES are almost always close to those of the upper layer. This similarity can be explained by the fact that the individual misfit functions with the quickest convergence toward the minimum energy point are those with a back-azimuth parallel or orthogonal to the fast orientation of the lower layer, as shown in Figure 7. The stacked misfit function is thus dominated by such events, which have splitting parameters similar to those of the top layer (because the *XKS* waves from these events only split when traveling through the top layer). The incomplete removal of energy on the corrected transverse component for events with nonparallel and nonorthogonal back-azimuth values is responsible for the relatively slow convergence toward the minimum (Fig. 7).

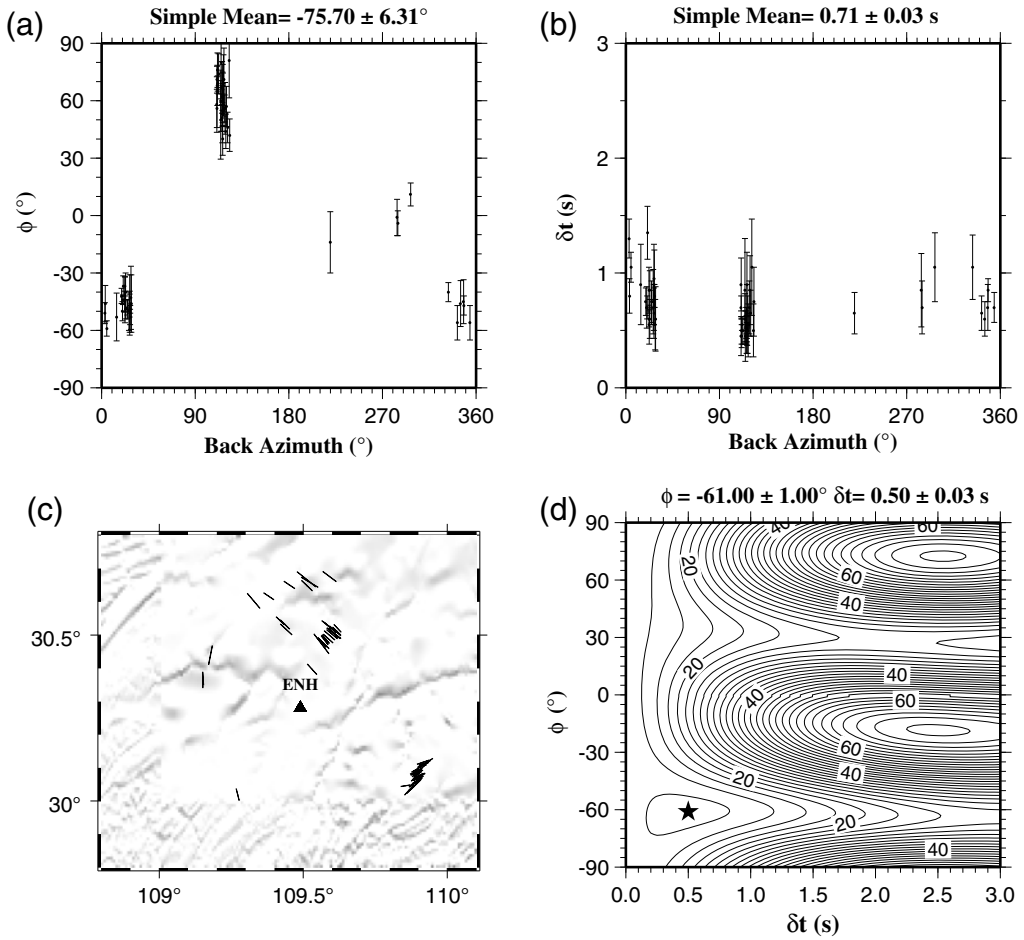

Figure 8. Results of shear-wave splitting (SWS) analysis using data recorded by station ENH in Hubei, China. (a) Fast orientations plotted against back azimuth. (b) Splitting times plotted against back azimuth. (c) Splitting parameters plotted above the ray-piercing points at 200 km depth. (d) Stacked misfit function and resulting optimal parameters using MES.

Testing Using Real Data

We next compare results from SC and MES using data recorded by two stations, one with laterally varying splitting parameters and one with periodic azimuthal variations of the splitting parameters that are indicative of multilayer anisotropy.

Apparent fast orientations obtained using SC from station ENH (Hubei, China) demonstrate strong azimuthal variations, but such variations are not periodic with either 90° or 180° periodicity (Fig. 8). They were interpreted as evidence for spatially varying simple anisotropy (Liu and Gao, 2013). The resulting δt from MES (0.5 s) is smaller than that from SC (0.71 s), a result that is consistent with the conclusions from synthetic tests using a model of spatially varying fast orientations (Fig. 3).

Station RES (Cornwallis Island, Canada) shows 90° periodic variations in the event-specific splitting parameters with respect to the back azimuth (Fig. 9). Under the assumption that the variations are associated with a two-layer model, we apply the technique of Silver and Savage (1994) to grid search for the optimal pairs of parameters for each of the two layers. Given the uneven back-azimuth distribution of the events, individual measurements are inversely weighted by the number of events in the back-azimuth range to which they belong before the grid searching. The results are 112° and 0.7 s for the upper layer and 76° and 0.35 s for the lower layer. Application of MES on data from the station led to a pair of optimal parameters (104°, 0.7 s) that are comparable with those of the upper layer, an observation that is consistent with the conclusion from synthetic tests that the resulting splitting parameters from MES are similar to those of the upper layer (Fig. 6).

Summary Remarks

MES has been used by numerous SWS studies to obtain a single pair of splitting parameters by stacking misfit functions from individual events. It is especially useful for stations with a limited amount of high-quality data. Synthetic tests and tests using the observed data presented above suggest that this technique should be applied with caution. Specifically, it should only be used when seismic anisotropy beneath a recording station can be represented by a single

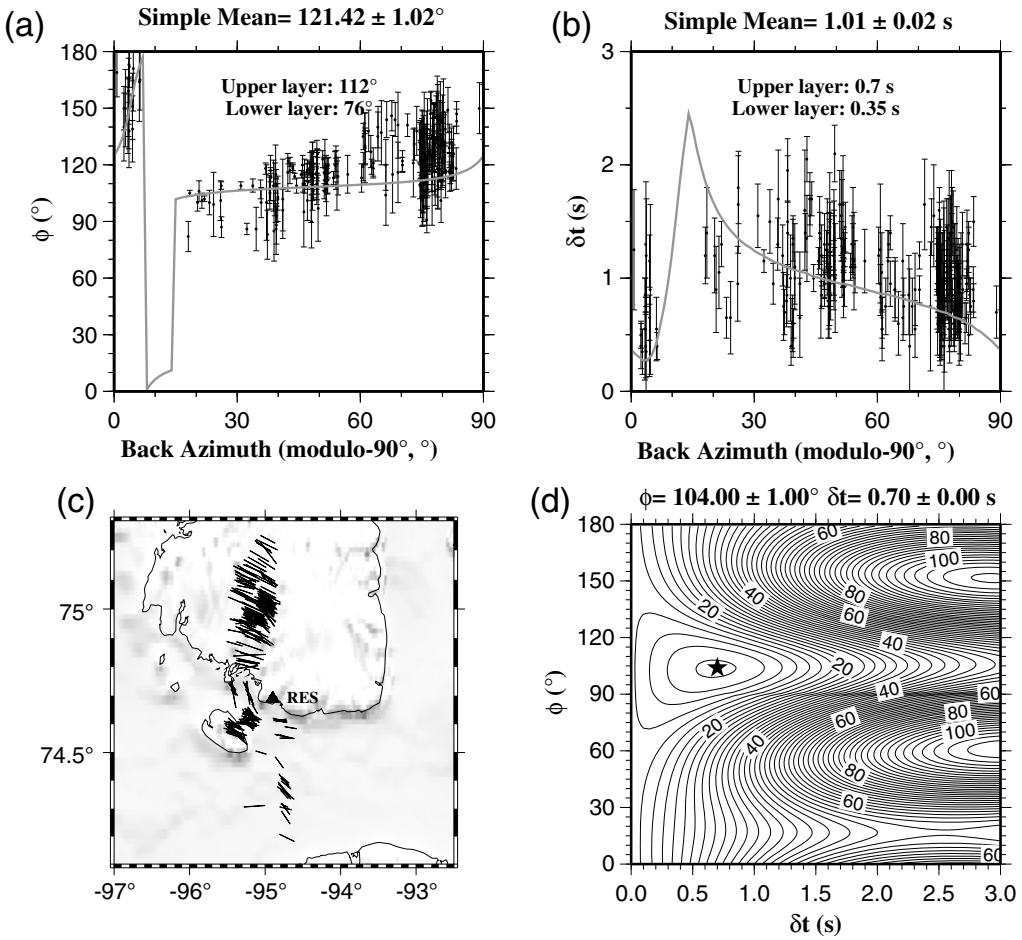

Figure 9. Same as Figure 8 but for station RES on Cornwallis Island, Canada. The solid lines in (a) and (b) are theoretical splitting parameters calculated using the splitting parameters from the two layers.

layer of anisotropy with a horizontal axis of symmetry and is characterized by azimuthally invariant fast orientations. Otherwise, conflicting implications might be obtained, especially when δt is used to constrain the anisotropy strength in studies involving geodynamic modeling or tomographic inversion (Becker, 2008; Yuan and Romanowicz, 2010).

To explore the existence of azimuthal variations of the individual fast orientations, high-quality *XKS* events in a wide back-azimuth band are needed. When such events are available at a station, SC can be used to obtain the splitting parameters from each of the events. If the individual fast orientations from SC are found to be azimuthally invariant, the individual measurements can safely be used to compute station-averaged splitting parameters without the need for MES. On the other hand, if systematic azimuthal variations are observed, complex anisotropy can be identified and possibly be characterized by grid searching or other approaches (e.g., Silver and Savage, 1994). Obviously, MES can still be used in areas with complex or spatially varying anisotropy to obtain reliable results by stacking events from narrow back-azimuthal windows (Bastow *et al.*, 2011), especially when limited amounts of high-quality data are present.

In summary, the study indicates that, although MES is a powerful tool for retrieving reliable splitting parameters of simple anisotropy with constant fast orientations, applying MES for areas with laterally varying fast orientations may lead to significantly underestimated splitting times. In addition, applying it for areas with two-layer anisotropy could result in a pair of splitting parameters resembling those of the top layer and not the actual anisotropic structure.

Data and Resources

Data recorded by stations ENH and RES were obtained from the Data Management Center of the Incorporated Research Institutions for Seismology (http://www.iris.edu/data/; last accessed September 2014). The data set is publicly accessible.

Acknowledgments

We thank two anonymous reviewers for constructive suggestions. The study was partially funded by the U.S. National Science Foundation under Award EAR-1009946 and by Statoil of Norway.

References

Alsina, D., and R. Snieder (1995). Small-scale sublithospheric continental mantle deformation: Constraints from SKS splitting observations, *Geophys. J. Int.* **123,** 431–448, doi: 10.1111/j.1365-246X.1995.tb06864.x.

Ando, M., Y. Ishikawa, and F. Yamazaki (1983). Shear wave polarization anisotropy in the upper mantle beneath Honshu, Japan, *J. Geophys. Res.* **88,** 5850–5864, doi: 10.1029/JB088iB07p05850.

Bai, L., T. Iidaka, H. Kawakatsu, Y. Morita, and N. Dzung (2009). Upper mantle anisotropy beneath Indochina block and adjacent regions from shear-wave splitting analysis of Vietnam broadband seismograph array data, *Phys. Earth Planet. In.* **176,** 33–43, doi: 10.1016/j.pepi.2009.03.008.

Bastow, I., D. Thompson, J. Wookey, J. Kendall, G. Helffrich, D. Snyder, D. Eaton, and F. Darbyshire (2011). Precambrian plate tectonics: Seismic evidence from northern Hudson Bay, Canada, *Geology* **39,** 91–94, doi: 10.1130/G31396.1.

Becker, T. W. (2008). Azimuthal seismic anisotropy constrains net rotation of the lithosphere, *Geophys. Res. Lett.* **35,** L05303, doi: 10.1029/2007GL032928.

Becker, T. W., S. Lebedev, and M. D. Long (2012). On the relationship between azimuthal anisotropy from shear wave splitting and surface wave tomography, *J. Geophys. Res.* **117,** no. B1, doi: 10.1029/2011JB008705.

Chevrot, S. (2000). Multichannel analysis of shear wave splitting, *J. Geophys. Res.* **105,** no. B9, 21,579–21,590, doi: 10.1029/2000JB900199.

Fuchs, K. (1977). Seismic anisotropy of the subcrustal lithosphere as evidence for dynamical processes in the upper mantle, *Geophys. J. Int.* **49,** 167–179, doi: 10.1111/j.1365-246X.1977.tb03707.x.

Gao, S. S., and K. H. Liu (2009). Significant seismic anisotropy beneath the southern Lhasa Terrane, Tibetan plateau, *Geochem. Geophys. Geosyst.* **10,** Q02008, doi: 10.1029/2008GC002227.

Gao, S. S., K. H. Liu, and M. G. Abdelsalam (2010). Seismic anisotropy beneath the Afar depression and adjacent areas: Implications for mantle flow, *J. Geophys. Res.* **115,** no. B12, doi: 10.1029/2009JB007141.

Levin, V., W. Menke, and J. Park (1999). Shear wave splitting in the Appalachians and the Urals: A case for multilayered anisotropy, *J. Geophys. Res.* **104,** 17,975–17,993, doi: 10.1029/1999JB900168.

Liu, K. H., and S. S. Gao (2013). Making reliable shear-wave splitting measurements, *Bull. Seismol. Soc. Am.* **103,** 2680–2693, doi: 10.1785/0120120355.

Liu, K. H., A. Elsheikh, A. Lemnifi, U. Purevsuren, M. Ray, H. Refayee, B. B. Yang, Y. Yu, and S. S. Gao (2014). A uniform database of teleseismic shear wave splitting measurements for the western and central United States, *Geochem. Geophys. Geosyst.* **15,** 2075–2085, doi: 10.1002/2014GC005267.

Long, M. D., and T. W. Becker (2010). Mantle dynamics and seismic anisotropy, *Earth Planet. Sci. Lett.* **297,** 341–354, doi: 10.1016/j.epsl.2010.06.036.

Press, W. H., S. A. Teukolsky, W. T. Vetterling, and B. P. Flannery (1992). *Numerical Recipes in FORTRAN*, Second Ed., Cambridge University Press, Cambridge, Massachusetts, 294 pp.

Restivo, A., and G. Helffrich (1999). Teleseismic shear wave splitting measurements in noisy environments, *Geophys. J. Int.* **137,** 821–830, doi: 10.1046/j.1365-246x.1999.00845.x.

Silver, P. G. (1996). Seismic anisotropy beneath the continents: Probing the depths of geology, *Annu. Rev. Earth Planet. Sci.* **24,** 385–432, doi: 10.1146/annurev.earth.24.1.385.

Silver, P. G., and W. W. Chan (1991). Shear wave splitting and subcontinental mantle deformation, *J. Geophys. Res.* **96,** 16,429–16,454.

Silver, P. G., and W. E. Holt (2002). The mantle flow field beneath western North America, *Science* **295,** 1054–1057, doi: 10.1126/science.1066878.

Silver, P. G., and M. K. Savage (1994). The interpretation of shear-wave splitting parameters in the presence of two anisotropic layers, *Geophys. J. Int.* **119,** 949–963, doi: 10.1111/j.1365-246X.1994.tb04027.x.

Vinnik, L. P., V. Farra, and B. Romanowicz (1989). Azimuthal anisotropy in the Earth from observations of SKS at Geoscope and NARS broadband stations, *Bull. Seismol. Soc. Am.* **79,** 1542–1558.

Walpole, J., J. Wookey, G. Masters, and J. M. Kendall (2014). A uniformly processed data set of SKS shear wave splitting measurements: A global investigation of upper mantle anisotropy beneath seismic stations, *Geochem. Geophys. Geosyst.* **15,** 1991–2010, doi: 10.1002/2014GC005278.

Wolfe, C. J., and P. G. Silver (1998). Seismic anisotropy of oceanic upper mantle: Shear wave splitting methodologies and observations, *J. Geophys. Res.* **103,** 749–771, doi: 10.1029/97JB02023.

Yang, B. B., S. S. Gao, K. H. Liu, A. A. Elsheikh, A. A. Lemnifi, H. A. Refayee, and Y. Yu (2014). Seismic anisotropy and mantle flow beneath the northern Great Plains of North America, *J. Geophys. Res.* **119,** 1971–1985, doi: 10.1002/2013JB010561.

Yuan, H., and B. Romanowicz (2010). Lithospheric layering in the North American craton, *Nature* **466,** 1063–1068, doi: 10.1038/nature09332.

Geology and Geophysics Program
Missouri University of Science and Technology
Rolla, Missouri 65409
fkd36@mst.edu
sgao@mst.edu
liukh@mst.edu

Manuscript received 25 August 2015;
Published Online 27 October 2015